

ECG6L: A Real Time Wireless Portable Six-Lead ECG

*Original*

ECG6L: A Real Time Wireless Portable Six-Lead ECG / Randazzo, Vincenzo; Sento, Marco; Pasero, Eros. -  
ELETTRONICO. - (2025), pp. 1-6. ( 2025 IEEE Medical Measurements & Applications (MeMeA) Chania (Gre) 28-30 May  
2025) [10.1109/memea65319.2025.11067984].

*Availability:*

This version is available at: 11583/3002111 since: 2025-07-25T16:14:23Z

*Publisher:*

IEEE

*Published*

DOI:10.1109/memea65319.2025.11067984

*Terms of use:*

This article is made available under terms and conditions as specified in the corresponding bibliographic description in the repository

*Publisher copyright*

IEEE postprint/Author's Accepted Manuscript

©2025 IEEE. Personal use of this material is permitted. Permission from IEEE must be obtained for all other uses, in any current or future media, including reprinting/republishing this material for advertising or promotional purposes, creating new collecting works, for resale or lists, or reuse of any copyrighted component of this work in other works.

(Article begins on next page)

# ECG6L: a real time wireless portable six-lead ECG

Vincenzo Randazzo  
*DET*  
Politecnico di Torino  
Turin, Italy  
vincenzo.randazzo@polito.it

Marco Sento  
*DET*  
Politecnico di Torino  
Turin, Italy  
marco.sento@polito.it

Eros Pasero  
*DET*  
Politecnico di Torino  
Turin, Italy  
eros.pasero@polito.it

**Abstract**—Cardiovascular diseases (CVDs) have significant impacts on health, quality of life and economics, being the major cause of death and disability worldwide. Also in Europe, CVDs are the leading cause of death, accounting for 45% of all deceases with an estimated cost of 210 billion of euros annually. Addressing CVDs through prevention and monitoring is crucial to improve health expectancy and reducing the economic burden of these diseases. Several devices allow for self monitoring of heart activity but many of them are not designed to provide a comprehensive diagnosis of cardiac conditions, commonly providing just numerical information about heart activity and, less frequently, reporting a single-lead electrocardiogram (ECG). This paper aims to present a portable device capable to overcome these limitations, delivering a six leads medical ECG in a non-invasive way. The combined use of digital and analog filtering of the signals acquired via three electrodes, made it possible to create a device capable of acquiring a high-quality six-lead ECG while maintaining an extremely compact design. The integration with the smartphone application allows the storing of ECG data for future analysis and references; moreover, the possibility of sharing data sets the basis for fast and efficient diagnosis of heart diseases.

**Index Terms**—Clinical diagnosis, Six-lead Electrocardiogram, Telemedicine, Uncertainty, portable devices

## I. INTRODUCTION

Cardiovascular diseases (CVDs) have become the leading cause of mortality worldwide, mainly due to changes in people's lifestyle and to an increasingly elder population. According to the World Health Organization (WHO), CVDs are responsible for approximately 17.8 million deaths each year, accounting for 32% of all premature deaths worldwide [1]. Even when non-fatal, CVDs cause long-term problems for patients, but not only: the impairing nature which characterises CVDs, as in the case of congenital heart diseases, causes a significant impact on the health care system, with an estimated cost, just for the European union, of 282 billion euros annually [2]. In addition to the economic implications, the need for patients to receive frequent check-ups poses additional problems: it contributes to saturation of waiting lists, compromising the efficiency of medical structures but, at the same time, it requires the provision of quality healthcare for all individuals, particularly difficult in remote and rural areas. According to WHO, almost 80% of CVDs deaths occur where access to effective and equitable healthcare is most difficult, such as in low- and middle-income countries [3].

Innovative solutions must therefore be sought in order to provide universal access to essential diagnostic tools, in an

equal and continuous manner, without further overburdening the healthcare system. It is well known that wearable devices have gained great popularity over the past 10 years, paving the way for remote patient monitoring. Wearable devices like smartwatches and fitness trackers enable real-time monitoring of vital signs, aiding doctors in providing continuous care through remote patient monitoring, reducing hospital visits and stays, easing healthcare system pressure, and helping to detect sporadic abnormalities often missed in occasional exams. However, it is necessary to provide to doctors information about parameters of real clinical utility and to ensure the reliability of these measures indeed, the large market for portable and wearable devices, characterised by poor quality measurements and lack of compliance with standards and certifications such as [4], undermines the credibility of these instruments.

An example of a consumer device capable of offering additional information compared to traditional devices is the Apple Watch Series 10 [5]. It is capable of acquiring a 30-second single-lead ECG trace and identifying certain conditions, including sinus rhythm and atrial fibrillation, demonstrating a specificity of 99.3% in the classification of the former condition and a sensitivity of 98.5% in the classification of the latter, in recordings that could be classified. However, no detailed data are reported in [6] regarding the differences in the morphology of the trace reported by the device compared to a reference wave, which is essential to attest the actual relevance of the instrument for doctors. Indeed, abnormalities are identified by visual inspection and pathological variations in the signal profile include absence of the P wave, a sinusoidal signal pattern, or even a "sawtooth" profile. Interpreting the information with the right scale is therefore crucial to identify even the smallest variation in the cardiac rhythm as is the case of ventricular hypertrophy. Nevertheless, the contribution of this device is relevant for its influence on public opinion, highlighting the potential of telemedicine to provide a solution for the remote monitoring of patients.

To overcome the presented challenges, this article proposes the ECG6L: a low-power, wireless, portable device able to acquire all limb leads used for medical diagnosis (I, II, III, aVL, aVR, aVF). Therefore, it provides a more complete overview of the heart's health state compared to commercial solutions. The combination of digital and analog filtering of the acquired signals made it possible to acquire a high quality

six-leads electrocardiogram maintaining an extremely compact design. Acquired data are then transmitted via Bluetooth, for wireless connectivity, so that the electrocardiogram can be visualized in real-time and eventually shared with doctors.

The intended use of the ECG6L is not for continuous monitoring, where the electrodes remain connected for extended periods (typically 24-72 hours), but rather for intermittent on-demand acquisitions. This approach has been shown to be effective [7] and responds to different clinical needs, monitoring the status of patients over the long term (weeks or months). This is useful, for example, during treatment with beta-blockers and the monitoring of prolonged events such as continuous extrasystoles and atrial fibrillation [8].

## II. THEORETICAL FRAMEWORK

The electrocardiogram (ECG) is a graphical representation of the heart's electrical activity over time. A single lead represents the variations of the potential difference between two points of the human body. The ECG waveform of a healthy patient shows typically 3 segments (P wave, QRS complex and T wave [9]), each of which represents a different aspect of the heart's electrical activity.

Portable and wearable devices usually display only numerical information such as the number of beats and the percentage of oxygen in the blood, without the possibility to appreciate the shape of the electrical or optical signals. In the above-mentioned case of [5] but also in the Vital-ECG [10], [11], and in the subsequent evolutions such as the ECG Watch [12], [13], realised by the research team led by Prof. Eros Gian Alessandro Pasero respectively in 2018 and 2019, a single lead representation of the electrocardiogram is shown.

A complete electrocardiogram analysis makes use of ten electrodes and is known as 12-lead ECG. In this setup, the subject lies supine, and the ten adhesive electrodes are placed on his chest and on his limbs. The changes in the heart's electrical potential are thus measured from twelve different angles, and recorded for a certain period, usually ten seconds. In this way, a complete overview of the heart's activity is captured during each phase of the cardiac cycle [14]. Therefore, a complete electrocardiogram involves wearing many electrodes and the use of specialised equipment that is as sophisticated as it is cumbersome, which is not a comfortable solution; moreover, it is characterised by signals belonging to two distinct groups of leads: limb leads and precordial leads. While the limb leads provide a general overview of the cardiac condition, the precordial leads are inspected for assessing the status of the left ventricle, and for their study it is mandatory to place the electrodes directly on the chest along the horizontal plane [14]. Although a 12-lead electrocardiogram provides a complete view of the state of health of the heart, allowing the identification of various pathologies, a six-lead ECG allows the immediate identification of abnormalities that cannot be seen on lead I alone, such as inversion of the cardiac axis, low peripheral voltages symptomatic of conditions such as obesity, chronic obstructive pulmonary disease or pulmonary

emphysema, severe hypothyroidism, diffuse necrosis, pericardial effusion and infiltrative pathologies (e.g. amyloidosis with cardiac involvement) [15], but also situations of myocardial ischaemia [16] that cannot be seen on lead I alone.

### A. Relationship between the acquired leads

The design of the conceived system allows the simultaneous acquisition of all the leads located on the frontal plane, exploiting the mathematical relationship between them; in fact, limb leads are further distinguished between the Einthoven's and Goldberger's leads. These derivations consist of six different signals, namely Lead I, II and III and augmented voltages aVF, aVR and aVL. Lead I compares the potential differences between two electrodes. Lead I compares the electrode on the left arm with the electrode on the right arm, where the former, observing from  $0^\circ$ , is at a lower potential. Lead II compares the left leg with the right arm, with the leg electrode being at a higher potential. Lead II observes the heart from an angle of  $60^\circ$ . Lead III compares the left leg with the left arm, with the leg electrode being the exploring one. It observes the heart from an angle of  $120^\circ$ . The spatial organization of these leads forms a triangle known as Einthoven's triangle [9] (see Fig. 1).

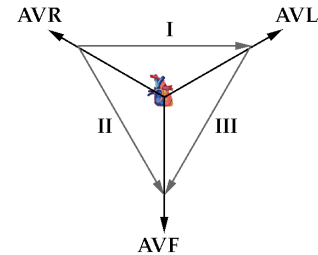


Fig. 1: ECG limb vectors.

Exploiting the mathematical relationship between the limbic signals, all limb leads can be acquired using just three electrodes placed on the right arm, the left arm and the left leg. The Einthoven's leads (leads I, II and III) are derived using only two derivations. The remaining 3 leads use a reference given by the average of the other three derivations, which is called the Goldberger's central terminal. With reference to the Einthoven's triangle (see Fig. 1), it is possible to define two vectors, derivations I and II, measuring the potential difference between the electrode placed on the right hand (RA), used as reference, and the electrodes of the left hand (LA) and the left leg (LL). On the other hand, the augmented voltages are obtained from a vector sum of the Einthoven's one. Considering, by definition, the reference potential at the

center of the heart, we can derive the Goldberger's leads:

$$\begin{aligned} aVL &= \frac{I - III}{2} \\ aVR &= -\frac{I + II}{2} \\ aVF &= \frac{II - III}{2} \end{aligned} \quad (1)$$

This shows that leads aVR, aVL and aVF can be calculated using just leads I, II and III. Therefore, these leads (aVF, aVR, aVL) do not offer any new information, but show it from different angles [17].

### III. DEVICE ARCHITECTURE

The proposed system, whose block diagram is shown in Fig. 2, consists of a portable device capable of providing a six-lead medical ECG in a non-invasive way. Energy efficiency is a major concern in order to guarantee a long operating autonomy; hence, the search for low-power integrated circuits. The battery is rechargeable via a C-type USB connector and the integration of the Bluetooth 5.3 transceiver, whose physical layer is already integrated in the microcontroller, enables efficient wireless communication with minimal power consumption, allowing data to be processed on the central device. This allows an accurate and reliable acquisition of a six-lead electrocardiogram, easily and in any context.

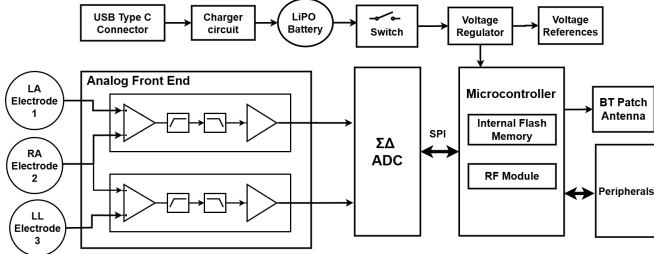


Fig. 2: Block diagram of the device.

The analog front end exploits three electrodes (LA, RA and LL) to acquire the ECG signal in a differential way. Each electrode measures 2 cm in diameter and 2 mm in height, and is made of copper; they are connected to the front end as shown in Fig. 2. Since they are used without conductive gel, this simplifies their daily use but results in a higher impedance than wet electrodes. For this reason, they are connected to the input of instrumentation amplifiers that allow the acquisition of the ECG signal without significant variations, in case of impedance variations due to different materials or oxidation. Two electrodes are placed on the front side of the prototype, named ECG6L from now on, on which the thumbs of the patient's right and left hand are placed. These two electrodes can be seen in Fig. 3 (left). A third electrode is placed on the lower part of the device and allows the lead between the right hand and left ankle to be acquired. As reported in Fig. 3 (right), this can be done by crossing the left leg during acquisition or by placing the device on the left iliac fossa for a more comfortable acquisition.



Fig. 3: ECG6L prototype (left) and usage (right).

The high CMRR of the instrumentation amplifier (110 dB), the isolated battery supply, and the filters offer sufficient rejection of RF noise, 50 Hz line noise, and muscle noise therefore it was possible to avoid the typically used right leg drive amplifier [18]. Signals are then band pass filtered through the combination of a high pass filter with the cut-off frequency at 0.5 Hz and a series of RC low pass filter cutting at 30 Hz. The use of high-order filters for noise rejection has been intentionally avoided to prevent the introduction of ringing artefacts, in the output signal, that overlap with the QRS complex and the T wave of the ECG, which can lead to incorrect diagnoses. Finally, they are amplified to optimize the signal to noise ratio (SNR) due to the quantization. The analog signals are then sampled with a 24 bit Sigma Delta analog-to-digital converter. Using an 8 MHz clock, the ADC is capable of simultaneously sampling the two differential channels, and thus the leads I and II, with a rate of 1300 Sps for each. The integrated circuit chosen for this operation is the Microhip MCP3564 since it offers the possibility of sampling the signals on 4 differential channels and iterating the acquisitions over a user-defined channel sequence, automating the acquisitions and increasing the throughput. The STM32WB30RG microcontroller embeds an ultra low power radio compliant with Bluetooth® LE 5.3 specifications. The current consumption of 5.2 mA in transmission over a personal area network, at 0 dBm of output power, the low cost, and the ability to reduce power consumption to 13 nA in shutdown mode, made it the optimal choice for a portable device. The circuit is powered from a Li-Polymer battery, regulated at 3.3 V by an inductor-less buck/boost switching regulator working at 1.5 MHz. The overall power consumption of the prototype depends on the frequency of electrocardiogram acquisitions. In particular, during the stand-by phase, the overall power consumption is only 80  $\mu$ W. During acquisition, the wake-up of the ICs and data transmission via Bluetooth LE results in a power demand of 100 mW. By powering the device with a 190 mAh rechargeable battery, capable of offering a nominal energy of 0.7 Wh, the standby autonomy is one year while with normal use, which consists of an acquisition of 30 s per hour, for eight hours a day, the duration of the device is 2.5 months.

Established the Bluetooth LE connection with the peripheral, it is possible to retrieve the ECG data and store them on the client for further processing. This initial step sets the basis for the subsequent digital signal processing (DSP) operations, enabling the reconstruction of the six different ECG signals from the two acquired from the peripheral. Having divided the samples into two distinct signals, Lead I and Lead II, it is possible to obtain the remaining signals: Lead III, aVL, aVR and aVF. This is done by applying the mathematical equations reported in (1) and by leveraging on the Kirchhoff's current law for a closed circuit. Once all six signals have been obtained, filtering can be applied to improve their representation. Various noise sources contribute to ECG signal distortion: powerline interference, muscle activity, electrode movement, and motion artifacts [19]. These disturbances can significantly degrade the signal quality and hinder accurate interpretation. Digital filtering algorithms offer the ability to selectively attenuate or eliminate unwanted noise components, offering a cleaner and more reliable ECG data. A notch filter is introduced to eliminate residual contributions of interference from the power supply in a frequency range already attenuated by analog filtering. Similarly, a low pass and a high pass digital filters have been introduced to reinforce the attenuation of noise outside of the band of interest.

#### IV. EXPERIMENTAL RESULTS

The measures reported by the device developed were compared with a standard patient monitor in order to ascertain its reliability. Various tests were carried out using an electrocardiogram signal generator to assess its repeatability; indeed, using the Fluke ProSim 3 Vital Sign Simulators [20], it was possible to simulate the ECG traces of healthy patients or with arrhythmia in a deterministic and repeatable manner. This made it possible to acquire the leads required for the purpose of analysis simultaneously with the GE Healthcare B105 patient monitor [21], a CE device used by technicians and doctors in clinics and hospitals.

The signals acquired for the comparison are the six limbic leads, reconstructed as discussed previously, using three electrodes, for both devices. Fig. 4 shows the result of the acquisition performed at 60 bpm without any cardiac anomalies: all the three peripheral leads, Lead I, Lead II, Lead III, have been acquired with both the devices; the figure is divided into six sections, one for each lead. Each of these plots shows the signal provided by the GE B105 on the left and the one acquired with the ECG6L on the right. From this preliminary comparison, it is possible to appreciate the consistency of the acquisitions performed by the two devices. Despite the extensive range of tools and literature available regarding electrocardiograms, evaluating ECG quality remains a challenging task, particularly from an analytical perspective. The visual inspection, although qualitative, is noteworthy as it constitutes the first diagnostic tool commonly used in clinical practice, complementing the measures reported hereafter.

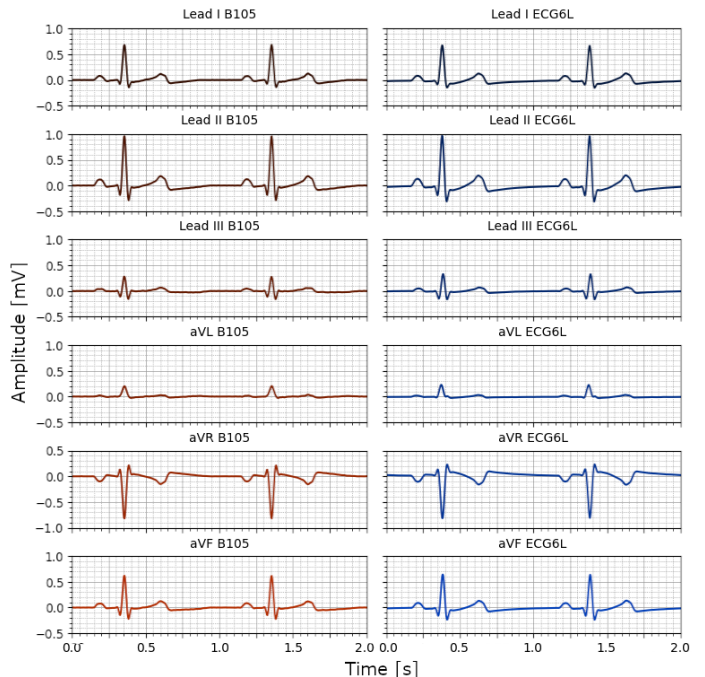


Fig. 4: Comparison of six-lead acquisition between GE B105 (red) and ECG6L (blue).

In the following, different metrics are used to evaluate ECG signals, both through time and frequency domain analysis. At first, the noise present on the input signals has been quantified. By acquiring a deterministic signal, it is possible to eliminate various noise contributions, such as those introduced by muscles and electrodes movements; however, the noise contribution of electromagnetic interference at 50 Hz remains dominant. The noise has been measured at the input of the circuit with a Rohde & Schwarz RTM3004 10-bit resolution oscilloscope, experimentally verifying a root mean square (RMS) value of 70.7 mV . Subsequently, the signal has been acquired with the device in the same nominal conditions, by applying the repeated-reading measurement method. The measurement was carried out by acquiring 50 PT segments of lead I, from which the RMS value of the applied input signal was obtained, which resulted in a value of 239  $\mu$ V . Considering the ratio of the RMS voltage of the signal ( $v_{RMS,s}$ ) to the RMS value of the noise voltage ( $v_{RMS,n}$ ), as shown in (2), the signal-to-noise ratio (SNR) of the input signal was then evaluated to be -49.4 dB .

$$\text{SNR}_{\text{dB}} = 20 \log_{10} \left( \frac{v_{RMS,s}}{v_{RMS,n}} \right) \quad (2)$$

In this way, it was also possible to quantify and attenuate the noise contributions of aleatory nature present on the signal acquired by the ECG6L, including the intrinsic uncertainty of the measurand, the internal noise of the acquisition chain and the instability of the state quantities of the system under measurement, as well as the residual input noise. The SNR obtained for the merely analogue-filtered signal has reported an average SNR of 29.8 dB , showing a noise attenuation of

about 80 dB . The further implementation of digital filters brings the SNR to 47.5 dB . This result shows a good repeatability of the measurements as well as a satisfactory rejection of the noises superimposed on the signal, offering an overall input noise attenuation of 97 dB .

To evaluate the similarity between the data from the GE B105 and the ECG6L acquired signals, the Root Mean Square Error (RMSE) has been selected as metric, considering the discrete characteristics of the signals. The RMSE represents the standard deviation of the residuals, the differences between reference values and the one provided by the prototype. Analysing a 10-second trace, it was possible to calculate the difference between the waveforms reported by the two devices: an RMSE of just 13.8  $\mu V$  was obtained, an average indication that can be considered as a deviation of just 1.6% for the peak value of the QRS complex or 6.9% of the T wave. In particular, a comparison of a complete cardiac cycle acquired from the Lead II is shown in Fig. 5, where it can be observed that the ECG6L curve (in blue) closely matches the GE B105 one (in red).

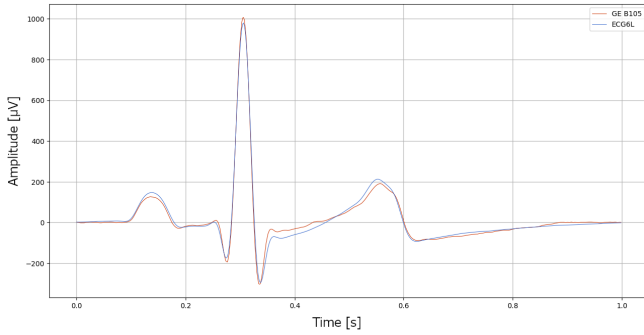


Fig. 5: Inspection of the two ECG complexes acquired, time (s) vs Amplitude ( $\mu V$ ): GE B105 (red), ECG6L (blue).

A more informative analysis is the measurement of several key parameters for the interpretation of an electrocardiogram. The analysis performed involved measuring the duration of the QRS complex, the R-R and the P-R intervals, relative to Lead II, as well as measuring the amplitude of the QRS complex for Leads I, II and III (from which the other leads are derived mathematically). These are the known parameters of the waveform generated by the [20], through which it was possible to verify the traceability of the measurements offered by the device. In particular, Table I shows the average values obtained with the ECG6L for these parameters in four different situations, at 60, 100, 140 and 180 beats per minute, respectively.

The ECG amplitudes specified for the reference waveform reported in the user manual of the FLuke ProSim 3 are expressed as percentage of the Lead II, from the baseline to the peak of the R wave, with a maximum variation of 2%. Other leads are proportional: Lead I is 70% of Lead II and Lead III 30% of it, uniformly distributed around the mean in a range of  $\pm 5\%$ . The acquired values of Lead I,II and III show respectively an experimental standard deviation of the sample

TABLE I: ECG6L waveform feature extraction.

BPM [bpm]	QRS [mV]	$\Delta t$ QRS [ms]	$\Delta t$ R-R [bpm]	$\Delta t$ P-R [s]
60	I 0.680 II 0.985 III 0.296	66	59.95	0.172
100	I 0.678 II 0.979 III 0.279	62	99.90	0.15
140	I 0.656 II 0.958 III 0.285	65	139.85	0.13
180	I 0.630 II 0.950 III 0.284	64	179.65	0.095

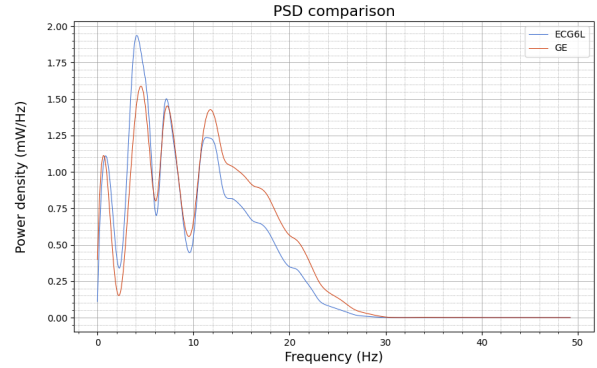


Fig. 6: PSDs of ECG6L (blue) and GE B105 (red).

of 2%, 1.5% and 3% relatively to the mean. Regarding the temporal metrics, the distance between two R-peaks admits a variation of 1% with respect to the nominal heart rate. In this case, the measurement of the cardiac frequency is accurate with a relative experimental deviation of 0.2%. The manual also reports the duration of the P-R and QRS strokes, nominally 160 ms and 80 ms, but without any uncertainty estimate or information on the measurement conditions.

Finally, to better appreciate the information carried out by the ECG signal, it is useful to exploit the Fourier transform. Typically, the frequency range of the electrocardiogram signal goes from 0.05 Hz up to 100 Hz, with most of the energy concentrated in the range from 0.5 Hz to 40 Hz, as reported in [22]. It can be noted that the power spectral density (PSD) of the ECG6L, shown in red in Fig. 6, is compliant with this requirement.

Although there are several techniques to estimate the PSD of a signal, this analysis employs the discrete Fourier transform (DFT) of the signal using the Welch method [23], which improves the PSD estimation by dividing the signal into  $K$  overlapping segments  $x_k(n)$  of length  $N$ , applying a window function  $w(n)$  to each segment and then calculating the DFT to evaluate the frequency spectrum at frequency  $f$ . In (3),  $N_w$  is the energy normalization factor and  $j$  is the imaginary unit.

$$\text{PSD}(f) = \frac{1}{KN_w} \sum_{k=1}^K \left| \sum_{n=0}^{N-1} w(n) x_k(n) e^{-j2\pi f n/N} \right|^2 \quad (3)$$

This analysis provides an insight into how the power of the leads is distributed over the various frequencies for both the devices, in particular, the standard deviation between the two signals, analysed in the range between 0 and 50 Hz, is only 0.15 mW/Hz. In Fig. 6 it is possible to appreciate the comparison between the PSD of the signals provided by the ECG6L (blue) and the GE B105 (red) for a signal of amplitude 1 mV and heart rate 60 bpm.

## V. CONCLUSIONS

The management of cardiovascular diseases is a complex process involving several different approaches, ranging from lifestyle modifications to pharmacological aid and invasive procedures. Lifestyle behaviours including a heart-healthy diet, regular exercise, smoking cessation and stress reduction are essential to prevent and manage CVDs.

One area in which significant action can be taken is in post-operative care and monitoring of at-risk patients, with solutions aimed at reducing the burden on the healthcare system. Easy-to-use monitoring tools are essential to achieve this goal and the device illustrated in this article, the ECG6L, represents a valid portable, wireless, low-cost and non-intrusive tool, which performs on-request six-lead ECG recording, anytime, anywhere, without the need to physically go to hospitals or cardiologists. Preliminary tests using a patient simulator, the Fluke ProSim 3, as reference, and a certified standard patient monitor, the GE Healthcare B105, showed the metrological traceability of the ECG6L in acquiring all six limb leads. This is confirmed by metrological measurements, either with the evaluation of the SNR, that highlighted a good rejection of the different noise sources, and with the RMSE and PSD metrics, which denote a high adherence to the reference signal. The current development involves the integration with all the services already developed by [10]–[13], such as the direct transmission of traces to medical personnel, the real time display of the ECG waveforms on the smartphone application and the analysis of plethysmography, as well as the functions already developed in the work [24] for the measurement of arterial blood pressure via neural networks. With the implementation, already in progress [25], of all the above-mentioned functionalities, it will therefore be possible to offer a valid and complete predictive and diagnostic tool for the autonomous monitoring of cardiovascular diseases.

Future works will further assess the quality of ECG6L by comparing it with different electrocardiographs and wearable commercial devices, as well as to by using additional evaluation metrics, such as the Bland-Altman plot and the Cumulative Spectral Power. Finally, it will be clinically tested on a cohort of patients with and without CVDs.

## REFERENCES

- [1] N. Townsend *et al.*, “Epidemiology of cardiovascular disease in Europe,” *Nature Reviews Cardiology*, vol. 19, no. 2, pp. 133–143, 2022.
- [2] R. Luengo-Fernandez *et al.*, “Economic burden of cardiovascular diseases in the European Union: a population-based cost study,” *European Heart Journal*, vol. 44, no. 45, pp. 4752–4767, 2023.
- [3] J. P. Ferreira *et al.*, “World Heart Federation roadmap for heart failure,” *Global Heart*, vol. 14, no. 3, pp. 197–214, 2019.
- [4] IEC 60601-1-11:2015/Amd 1:2020: *Medical electrical equipment - Part 1-11: General requirements for basic safety and essential performance - Collateral standard: Requirements for medical electrical equipment and medical electrical systems used in the home healthcare environment*, International Electrotechnical Commission Std., 2020.
- [5] Apple Inc., “Eu declaration of conformity for apple watch series 10,” Available online at <https://regulatoryinfo.apple.com/en/eurocompliance>, 2024.
- [6] Apple Inc., “User instructions for ecg global 2.0 app,” Available online at <https://www.apple.com>, One Apple Park Way, Cupertino, CA 95014, USA, 2024.
- [7] P. S. Doliwa, M. Rosenqvist, and V. Frykman, “Paroxysmal atrial fibrillation with silent episodes: Intermittent versus continuous monitoring,” *Scandinavian Cardiovascular Journal*, vol. 46, no. 3, p. 144–148, 2012.
- [8] T. Hendrikx, M. Rosenqvist, P. Wester, H. Sandström, and R. Hörnsten, “Intermittent short ecg recording is more effective than 24-hour holter ecg in detection of arrhythmias,” *BMC Cardiovascular Disorders*, vol. 14, no. 1, 2014.
- [9] S. Meek and F. Morris, “Abc of clinical electrocardiography: Introduction. i—leads, rate, rhythm, and cardiac axis,” *BMJ*, vol. 324, no. 7334, p. 415–418, 2002.
- [10] V. Randazzo, J. Ferretti, and E. Pasero, “A wearable smart device to monitor multiple vital parameters—vital ecg,” *Electronics*, vol. 9, no. 2, 2020. [Online]. Available: <https://www.mdpi.com/2079-9292/9/2/300>
- [11] V. Randazzo, E. Pasero, and S. Navaretti, “Vital-ecg: A portable wearable hospital,” in *2018 IEEE Sensors Applications Symposium (SAS)*, 2018, pp. 1–6.
- [12] V. Randazzo, J. Ferretti, and E. Pasero, “Anytime ecg monitoring through the use of a low-cost, user-friendly, wearable device,” *Sensors*, vol. 21, no. 18, 2021. [Online]. Available: <https://www.mdpi.com/1424-8220/21/18/6036>
- [13] V. Randazzo, J. Ferretti, and E. Pasero, “Ecg watch: a real time wireless wearable ecg,” in *2019 IEEE International Symposium on Medical Measurements and Applications (MeMeA)*. IEEE, 2019, pp. 1–6.
- [14] P. Macfarlane and E. Coleman, “Resting 12-lead electrode,” *Society for Cardiological Science and Technology*, 1995.
- [15] F. Gibiino, F. Sanguetoli, and F. Vitali, “Quando l’ecg non vede l’ipertrofia,” *Giornale Italiano di Cardiologia*, vol. 23, no. 3, p. 172, 3 2022. [Online]. Available: <http://dx.doi.org/10.1714/3751.37335>
- [16] A. Coppolino and L. Valeri, “Dispnea e onde t negative diffuse: ischemia o altro?” *Giornale Italiano di Cardiologia*, vol. 22, no. 4, p. 276, 4 2021. [Online]. Available: <http://dx.doi.org/10.1714/3574.35572>
- [17] F. Gaita, J. Leclercq, L. Biasco, Y. Cristoforetti, and L. Garberoglio, *L’interpretazione dell’ECG. Un metodo semplice in 101 tracciati*. Edizioni Minerva Medica, 01 2012.
- [18] B. B. Winter and J. G. Webster, “Driven-right-leg circuit design,” *IEEE Transactions on Biomedical Engineering*, vol. BME-30, no. 1, pp. 62–66, 1983.
- [19] R. Kher *et al.*, “Signal processing techniques for removing noise from ecg signals,” *J. Biomed. Eng. Res.*, vol. 3, no. 101, pp. 1–9, 2019.
- [20] Fluke Biomedical, *ProSim™ 2/3 Vital Signs Simulator Users Manual*, Available online at [https://www.flukebiomedical.com/sites/default/files/resources/prosim3\\_umeng0100\\_0.pdf](https://www.flukebiomedical.com/sites/default/files/resources/prosim3_umeng0100_0.pdf), 2013.
- [21] GE HealthCare (United States), “B105 and b125 patient monitors,” Available online at <https://www.gehealthcare.com/products/patient-monitoring/patient-monitors/b105-and-b125-patient-monitors>, 2024.
- [22] N. V. Thakor, J. G. Webster, and W. J. Tompkins, “Estimation of qrs complex power spectra for design of a qrs filter,” *IEEE Transactions on Biomedical Engineering*, vol. BME-31, no. 11, pp. 702–706, 1984.
- [23] P. Welch, “The use of fast fourier transform for the estimation of power spectra: A method based on time averaging over short, modified periodograms,” *IEEE Transactions on Audio and Electroacoustics*, vol. 15, no. 2, pp. 70–73, 1967.
- [24] A. Paviglianiti, V. Randazzo, S. Villata, G. Cirrincione, and E. Pasero, “A comparison of deep learning techniques for arterial blood pressure prediction,” *Cognitive computation.*, vol. 14, no. 5, 2022-09.
- [25] V. Randazzo, P. Buccellato, J. Ferretti, F. Delrio, and E. Pasero, “Pulsecg—a cuffless non-invasive blood pressure monitoring device through neural network analysis of ecg and ppg signals,” in *2024 IEEE 22nd Mediterranean Electrotechnical Conference (MELECON)*. IEEE, 2024, pp. 1030–1035.